Journal of Catalysis **202,** 1–13 (2001)
doi:10.1006/jcat.2001.3270, available online at http://www.idealibrary.com on IDEAL®

Isobutane Dehydrogenation over Supported Platinum Acid–Base AlGaPON Catalysts

S. Delsarte,* F. Maugé,† and P. Grange*,[1]

Catalyse et chimie des matériaux divisés, Université catholique de Louvain, Croix du Sud 2/17, 1348 Louvain-la-Neuve, Belgium; and †Laboratoire de Catalyse et Spectrochimie, URA CNRS 414, ISMRA Université, 6 Boulevard du Maréchal Juin, 14050 Caen Cedex, France

Received July 20, 2000; revised March 12, 2001; accepted April 28, 2001

Isobutane dehydrogenation was studied on platinum impregnated galloaluminophosphate AlGaPO and nitrided galloaluminophosphates AlGaPON, in a conventional continuous flow microreactor system at 500°C. By comparison with AlPO(N), it is shown that gallium plays an important role in the catalytic process by increasing the selectivity of the transformation for isobutene. An isobutene yield of 62% was obtained for a platinum impregnated AlGaPON sample containing 11.8 wt%N, whereas the platinum impregnated precursor AlGaPO only converts isobutane to isobutene with a yield of 49% under similar reaction conditions. This indicates the participation of the basic sites, created by nitridation, to the catalytic conversion of isobutane on Pt/AlGaPON. Both catalysts deactivate with time on stream, due to the deposition of carbonaceous species on the surface, but the activity decay is delayed on the less acid nitrided samples.

Key Words: **oxynitrides; galloaluminophosphates; FTIR of H_2 adsorption; isobutane dehydrogenation; acid–base catalysts.**

---

1. INTRODUCTION

The catalytic dehydrogenation of alkanes is a process of considerable importance because it represents a route for obtaining alkene from poorly reactive and low-cost saturated feedstocks. An important reaction, in this aspect, is the dehydrogenation of isobutane to isobutene. There is indeed an important market for this product: in 1996, a total of about 1.93 million tons of isobutene were consumed in Western Europe, not including refinery operations such as alkylation and polygasoline. Sixty four percent of the total demand concerned the production of methyl-t-butyl ether (MTBE), an oxygenated product used as an additive to reformulated gasoline. Butyl rubber and polyisobutylene were responsible for a further 28% of the demand and the remainder were specialities, e.g., antioxidants and peroxides (1). However, forecast concerning the future demand for isobutene should take into account recent concerns about the toxic effect of MTBE on human health (2).

A number of catalytic dehydrogenation processes are available today, whose characteristics were summarized in Ref. (3). Catalyst systems in those processes are either platinum-based catalysts or chromia-based catalysts. Although chromia is generally supported on alumina for industrial applications, zirconium dioxide has recently been the focus of some attention as a support, since it is highly stable thermally and only weakly acidic (4).

Commercially, the dehydrogenation of organic molecules is performed at high temperature (550–600°C), because of thermodynamic restrictions, and as a result, all available processes are facing limitations in terms of deactivation rate and yield. It seems that only a new generation of better catalysts could allow substantial improvements in dehydrogenation process performance (3).

One way of increasing the dehydrogenation catalytic activity of platinum-supported catalysts is to modify the acidity/alkalinity of the support. The reason is that acidity favors cracking and isomerization reactions (5), and it has a detrimental effect on catalyst life because the support acidity promoting coke formation under dehydrogenation conditions (6). In that sense for instance, Imai and Hung presenting an alumina-supported Pt/Sn/K catalyst for dehydrogenation reactions suggest the use of nonacidic supports to inhibit cracking and isomerization side reactions (7). They recommend decreasing the support acidity either by neutralizing the acid sites by potassium addition or by treating the catalyst with steam to remove the halogen contaminants.

Besides, it is known (8) that dehydrogenation reactions benefit from the existence of acid–base site pairs of intermediate strength, because such sites can form, stabilize, and discard adsorbed intermediates during a catalytic turnover.

Hence, it was decided to use solid oxynitrides with tuneable acid–base properties as support for platinum in the dehydrogenation of isobutane to isobutene. In a first step, nitrided aluminophosphates AlPON were used. Those solids are obtained by nitridation under ammonia flow of reactive

---

[1] To whom correspondence should be addressed. E-mail: grange@cata.ucl.ac.be.

amorphous $AlPO_4$ phosphate precursors (9). This treatment allows one to adjust their acid–base properties (10, 11) and to obtain a new family of solids where weakly acid sites are juxtaposed to weakly basic sites.

Preliminary studies showed that the Pt/AlPON were good dehydrogenation catalysts, presenting high conversions while keeping the isobutene selectivity at a relatively high level during the reaction (12, 13). In the present study, we present the catalytic properties of another oxynitride family, the nitrided galloaluminophosphates AlGaPON.

Gallium was chosen as a substituent of aluminum in AlGaPON because it is known to catalyze the rate-limiting dehydrogenation step during the conversion of alkanes to aromatics on modified H-ZSM5 zeolites (14). It is effective, whether in the impregnated form, in the ion-exchanged form, in the physically mixed form, or even when it is incorporated in the zeolite framework (15). Research in this field has led to the development by British Petroleum and UOP of the CYCLAR process for the conversion of light alkanes to aromatics (16).

We intend to present the role of gallium and nitrogen on the catalytic properties of the Pt/AlGaPON by comparing the activities of nonsupported alumino- and galloaluminophosphates AlPO and AlGaPO, as well as the activities of platinum-supported oxide and oxynitride samples. Experiments with different hydrogen partial pressures have been performed on a Pt/AlGaPON sample along with combined carbon analysis, in order to gather information on the dependence of the catalyst activity, selectivity, and stability on the hydrogen partial pressure in the feed.

2. METHODS

2.1. Materials

The $AlPO_4$ and $Al_{0.5}Ga_{0.5}PO_4$ phosphates were prepared by soft chemistry routes. The $AlPO_4$ was synthesised using the citric acid complexation method (17), whereas the mixed galloaluminophosphate $Al_{0.5}Ga_{0.5}PO_4$ was obtained by the method developed by Kearby (18) for $AlPO_4$ and adapted for (Al, Ga)PO compositions (19). The $Al_{0.5}Ga_{0.5}PO_xN_y$ oxynitrides were obtained by nitridation of the amorphous $Al_{0.5}Ga_{0.5}PO_4$ precursor at 750°C in a tubular furnace.

The platinum-impregnated samples were obtained by wet impregnation methods.

1. The $Al_{0.5}Ga_{0.5}PO_{2.23}N_{1.18}$ (AlGaPON2) sample was impregnated with a purely methanolic solution of $H_2PtCl_6 \cdot 6H_2O$ according to the procedure used in the preliminary studies on Pt/AlPON (12, 13): 0.0797 g of $H_2PtCl_6 \cdot 6H_2O$ (Merck) was dissolved in 50 ml of methanol (HPLC grade), then 2 g of AlGaPON powder was added and the mixture was kept at room temperature under mechanical stirring for 20 h. The excess solvent was removed under vacuum at room temperature, and the sample was then dried at 110°C overnight. The salt was decomposed under nitrogen flow (Air liquide, N28) with a ramp of 2°C/min up to 150°C, then 3°C/min up to 500°C and held at that temperature for 1 h, after which the sample was reduced in pure hydrogen (Air liquide, N40) at the same temperature during 2 h.
2. The $AlPO_4$, $Al_{0.5}Ga_{0.5}PO_4$, and $Al_{0.5}Ga_{0.5}PO_{2.46}N_{1.03}$ (AlGaPON1) samples were impregnated with a $(NH_3)_4Pt(NO_3)_2$ solution: 0.0595 g of $(NH_3)_4Pt(NO_3)_2$ (Aldrich) was dissolved in 2 ml of distilled water and 48 ml of methanol (HPLC grade) was added to the solution, then, 2 g of Al(Ga)PO(N) powder was added and the mixture was kept at room temperature under mechanical stirring for 20 h. After impregnation, the excess solvent was removed under vacuum at room temperature first, then for 15 min at 50°C. The samples were heated under nitrogen flow (Indugas, 5.0) with a ramp of 2.5°C/min up to 120°C and left for 2 h at that temperature then up to 350°C and left for 2 h at that temperature. Platinum was then reduced for 2 h under pure hydrogen flow (Air liquide, N40) at 500°C.

The platinum salts were decomposed under nitrogen rather than oxygen to avoid the substitution of nitrogen by oxygen (in a reaction inverse to nitridation), that would greatly modify the support characteristics.

In both cases, the amount of platinum impregnated is equivalent to 0.015 g platinum metal per gram of catalyst.

2.2. Physicochemical Characterizations

The amount of platinum after the impregnation procedure was determined by plasma emission spectroscopy (ICP-AES Philips PV8490 equipped with PV8250 spectrometer).

The nitrogen content of the samples was determined from the chemical dosage of nitrogen in a LECO elemental analyser equipped with a TC-36 program and an EF-400 oven.

The amount of carbon deposited on the surface at the end of the catalytic tests was measured in a Multilab CS-Analyser.

The specific surface areas of the samples were measured by the single-point BET method, in a Micromeritics Flowsorb II 2300 apparatus, after 120 min degasification at 150°C.

The metal dispersions were determined by CO chemisorption at 25°C in a Micromeritics Pulse Chemisorb 2700 apparatus. The number of platinum atoms exposed was determined supposing a stoechiometry factor of 1CO-1 atom of platinum. The use of this stoechiometry factor implies that CO is adsorbed over platinum in the linear Pt–CO form. This assumption is derived from an IR study of adsorbed CO carried out on the platinum impregnated samples.

The amount of surface acid sites on the catalyst surface was determined by temperature-programmed desorption of ammonia, using a “dynamic flow fixed bed”-type reactor and a procedure described previously (20). Ammonia is adsorbed on the surface at 100°C and progressively removed by increasing the temperature at 10°C/min under helium flow up to 700°C. The liberated ammonia is collected in a receiving flask containing a 10 g/l boric acid solution and titrated by 0.01N sulphuric acid.

2.3. FTIR Study of Hydrogen and Deuterium Adsorption

Transmission infrared spectra were recorded on a Nicolet 710 Fourier transform IR spectrometer. The powders were pressed into self-supporting disks (≈15 mg, 16 mm in diameter), placed in an IR cell connected to a vacuum line.

The samples were progressively (8°C/min) heated under vacuum at 500°C and left for 15 min at that temperature, after which a spectrum was recorded. Then, the samples were reduced at 500°C for 135 min under static conditions ($P_{H2} = 0.16$ atm) ($1 \text{ atm} = 1.013 \times 10^5$ Pa) with regular hydrogen renewals. They were again evacuated for 30 min at the same temperature and 30 min at RT, prior to the recording of a second spectrum.

Hydrogen–deuterium exchange experiments were conducted at 500°C on an AlGaPON oxynitride containing 10.8 wt%N: the sample was heated for 45 min under 0.16 atm of hydrogen, after which an IR spectrum was recorded. Hydrogen was then evacuated and replaced by 0.16 atm of deuterium for 45 min before the recording of a second spectrum. Finally, deuterium was evacuated and the sample again put in equilibrium with 0.16 atm of hydrogen for 45 min and a third spectrum was recorded.

2.5. Procedure for Activity Measurements

Before each test, and in order to secure a total reduction of platinum, the catalysts were heated (2.5°C/min) under a 5% H_2 in He flow of approximately 20 ml/min up to 500°C and left at that temperature for 1 h. Then, the samples were brought to the reaction temperature, and the reaction started by switching to a mixture of isobutane, hydrogen and helium. Initial activities were determined after 2 min of reaction.

The flow rates, set by using mass flow controllers, led to weight hourly space velocities (WHSV) of 0.03 and 0.55 h^{-1} at 25°C.

Hydrogen was added to the feed in order to avoid coke formation and catalyst deactivation. Unless stated otherwise, the isobutane/hydrogen ratio was 1/6.

The experimental conditions for the catalytic tests conducted with an isobutane/hydrogen ration of 1/6 are the following:

WHSV (h^{-1})	catalyst weight (mg)	hydrogen in helium flow		iC_4H_{10} in helium flow	
0.03	180	1% H_2	21.0 ml/min	1% iC_4H_{10}	3.5 ml/min
0.55	75	5% H_2	34.8 ml/min	5% iC_4H_{10}	5.8 ml/min

Under those experimental conditions, no reaction spontaneously occurs below 630°C.

The isobutane conversion (%) is calculated as follows:

$$\frac{\left(\left(\sum \text{of the peak areas of all the detected products}\right)_t - (\text{isobutane peak area})_t\right) \times 100}{\left(\sum \text{of the peak areas of all the detected products}\right)_t}$$

2.4. Catalysis Line and Gases

The catalysts, diluted with inert SiC particles, were tested in a conventional continuous flow microreactor system (internal diameter of 12 mm) operating at atmospheric pressure. The effluents of the reactor were analyzed by an online Packard (model 428) gas chromatograph equipped with flame ionisation detector, with helium as carrier gas. A 50 m × 0.32 mm (Chrompack, plot fused silica, Al_2O_3/KCl coating) capillary column was used for the separation of the various compounds.

The gases used were isobutane in helium (Air liquide, isobutane N35 in helium N50), hydrogen in helium (Air liquide, hydrogen N40 in helium N50) or pure hydrogen (Air liquide, hydrogen N40).

Before each analysis, the reactor was by-passed and the area of the isobutane peak measured after injection of the reactant mixture was recorded. Unless stated otherwise, the relative difference between this measurement and the sum of the peak areas of all the detected products after passage of the reactant mixture on the catalysts did not exceed 3.5%.

Selectivities are defined as the weight fraction of the reacted isobutane that is converted into a given product.

The yield for a product, expressed in percent, is the multiplication of the selectivity (%) by the total conversion (%) divided by 100.

For quantitative comparisons between catalysts, care was taken to ensure that the data were controlled neither by external nor by internal diffusion.

3. RESULTS

3.1. Sample Characteristics

The characteristics of both oxide and oxynitride supports, evaluated prior to platinum impregnation, are reported in Table 1. The chemical formulas for the oxynitride solids were established from the evaluation of the nitrogen content, assuming the replacement of 3 oxygen atoms by 2 nitrogen atoms during nitridation.

X-ray diffraction patterns of the AlPO and AlGaPO precursors show that they are amorphous. The two AlGaPON samples, obtained by nitridation at 750°C of the AlGaPO precursors are also amorphous.

Table 2 presents the characteristics of the impregnated catalysts, measured after impregnation and reduction of the samples. Samples 5–7 were impregnated in a water/methanol/$(NH_3)_4Pt(NO_3)_2$ solution, while sample 8 was impregnated in a purely methanolic solution of $H_2PtCl_{16} \cdot 6H_2O$. As evidenced in this table, the impregnation procedure induces a surface area decrease of roughly 15–20% and, for the nitrided samples, a decrease of the nitrogen content. The nitrogen loss is however strongly reduced when impregnating the samples in pure methanol (sample 8) rather than in a mixture of methanol and water (sample 7).

The important nitrogen loss observed for the AlGaPON1 sample impregnated in the presence of water could be caused by the high sensitivity of the nitrided phosphates toward hydrolysis.

The sensitivity of the nitrided phosphates toward hydrolysis was demonstrated by placing an AlPON sample in the presence of gaseous water in an *in situ* DRIFTS cell (21). This experiment showed that the AlPON undergoes hydrolysis even when the concentration of water in the gas phase is as low as 3 ppm. Hydrolysis transforms part of the bulk N^{3-} ions into surface hydrogenated nitrogen species NH_x, which can be easily removed from the surface.

Platinum dispersions attain 10% in the case of the platinum impregnated AlPO (sample 5) but are very low (<5%) on gallium-containing samples (samples 6–8). This indicates that the platinum impregnation procedure should be modified and improved in the future, which implies a fundamental study of the interactions between the platinum salts and those nonconventional supports in an alcoholic solvent.

3.2. FTIR Study of Hydrogen and Deuterium Adsorption

Figure 1 presents the IR spectra recorded in the [2100–2020 cm^{-1}] and [2550–2450 cm^{-1}] energy ranges on the AlGaPON1 sample evacuated at 500°C and reduced for 135 min under 0.16 atm of hydrogen at the same temperature. The *in situ* reduction of this sample induces the appearance of two bands, at 2055 (Fig. 1A) and 2510 cm^{-1} (Fig. 1B). Those bands are also visible, after exposure to hydrogen, on the platinum impregnated sample Pt/AlGaPON1 (Figs. 1A and 1B) and on the platinum impregnated Pt/AlGaPO sample (not shown).

When hydrogen is replaced by deuterium at 500°C, the two bands are shifted toward lower wavenumbers: the band at 2055 cm^{-1} is shifted at 1478 cm^{-1}; the band at 2510 cm^{-1} is shifted at 1820 cm^{-1} (Fig. 2). This replacement is reversible and the initial spectrum is restored after the evacuation of deuterium and its replacement by hydrogen for 45 min at 500°C.

3.3. Catalytic Properties

3.3.1. Isobutane Dehydrogenation on Nonimpregnated Samples

The catalytic properties of the nonimpregnated AlPO and AlGaPO samples were investigated as a function of temperature at a weight hourly space velocity of 0.03 h^{-1}. The samples were progressively heated under a 1% H_2 in He flow from 350 to 550°C and the catalytic activity measured every 50°C after temperature stabilisation. Under these conditions, and up to temperatures of 550°C, the AlPO sample is totally inactive. On the other hand, the gallium-containing sample converts isobutane to isobutene, and its activity increases with the temperature.

Figure 3 gives the evolution of the conversions and isobutene selectivities over the AlGaPO sample when the reaction temperature increases. Conversion measured for the AlGaPO precursor reaches 15% at 500°C, with a selectivity for isobutene of 98%. At 550°C, the conversion reaches 28%, with a selectivity for isobutene of 87%.

TABLE 1

Physicochemical Characterization of the Nonimpregnated Samples

Number	Name	Composition	S_{BET} (m^2/g)	Nitrogen content (wt%)	Acidity ($\mu eq./m^2$)
1	AlPO	$AlPO_4$	225	0	6.1
2	AlGaPO	$Al_{0.5}Ga_{0.5}PO_4$	315	0	7.7
3	AlGaPON1	$Al_{0.5}Ga_{0.5}PO_{2.46}N_{1.03}$	196	10.8	3.2
4	AlGaPON2	$Al_{0.5}Ga_{0.5}PO_{2.23}N_{1.18}$	146	12.6	2.3

TABLE 2

Physicochemical Characterization of the Platinum-Impregnated Samples

Number	Name	S_{BET} ($\mathrm{m^2/g}$)	Nitrogen content (wt%)	Nitrogen loss (%)	Platinum content (wt%)	Dispersion (%)
5	Pt/AlPO	195	—	—	0.9	10.5
6	Pt/AlGaPO	224	—	—	1.2	1.3
7	Pt/AlGaPON1	154	5.6	48	1.3	4.3
8	Pt/AlGaPON2	128	11.8	6	1.3	1.9

3.3.2. Isobutane Dehydrogenation on Platinum-Impregnated Samples

Influence of the temperature and Pt particles. Figure 4 shows the evolution of the conversions, as a function of temperature at a space velocity of 0.03 $\mathrm{h^{-1}}$ for the Pt/AlPO and Pt/AlGaPO samples. Platinum impregnation considerably modifies the catalytic properties: it makes the AlPO active and considerably increases the catalytic activity of the AlGaPO.

When the temperature reaches 500°C, the Pt/AlPO converts 44% of isobutane (with a very low selectivity to isobutene of 36%), while the AlPO is completely inactive under similar reaction conditions. The AlGaPO, which converted 15% of the isobutane at 500°C, converts 93% of isobutane (with a selectivity to isobutene of 77%) when it is impregnated with platinum. For both samples, a mass balance defect is observed: the area of the isobutane peak measured when the reactor is by-passed differs significantly from the sum of the peak areas of all the detected products after passage of the reactant mixture on the catalysts. The relative difference is of 15% for the Pt/AlPO sample and of 11% for the Pt/AlGaPO sample. This, most probably, is because at those high contact times, formation of a carbonaceous deposit on the surface causes errors in the mass balance.

The evolution of the conversion as a function of temperature was also recorded for the Pt/AlGaPON1 sample: the conversion profile obtained for this sample is similar to the profile obtained for the Pt/AlGaPO sample. At 500°C, the isobutane conversion measured for Pt/AlGaPO is equal to 93%, the conversion measured for the Pt/AlGaPON1 sample is 95%.

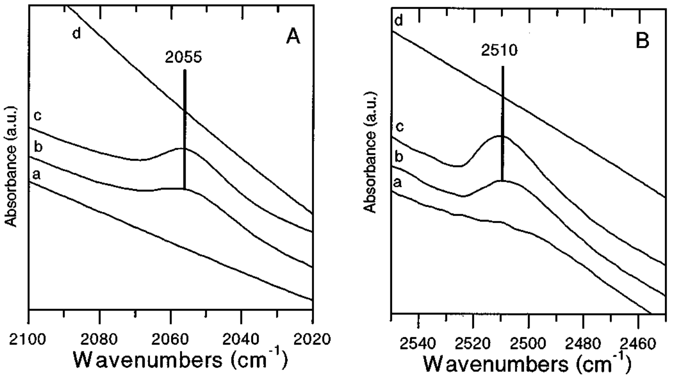

FIG. 1. FTIR spectra of the (a) AlGaPON1 oxynitride evacuated at 500°C and the (b) spectra of the AlGaPON1, (c) Pt/AlGaPON1 and (d) Pt/AlPON samples after heating under hydrogen at 500°C. Spectra are displayed in two regions: (A) 2100–2020 $\mathrm{cm^{-1}}$ and (B) 2550–2450 $\mathrm{cm^{-1}}$.

The thermodynamic equilibrium values were calculated taking into account the isobutane/isobutene equilibrium, the isobutane/hydrogen ratio of 1/6 and the dilution of the reactants with helium. Results are presented in Fig. 4. At 500°C, the calculated conversion at the thermodynamic equilibrium is 92%. Although the calculation did not take into account the formation of the by-products which appear under our reaction conditions, one can note that the conversions attained on the Pt/AlGaPO and Pt/AlGaPON1 samples are very close to the calculated conversions. This suggests that comparing the catalytic properties of those two samples necessitates working at a higher weight hourly space velocity, in order to decrease the contact times and to work below the thermodynamic equilibrium.

It is worth mentioning however that during the tests conducted at a WHSV of 0.03 $\mathrm{h^{-1}}$ on the platinum impregnated AlGaPON samples, a malodorous yellow deposit appeared on the cold part of the quartz microreactor. It was dissolved in acetone and analyzed by mass spectrometry.

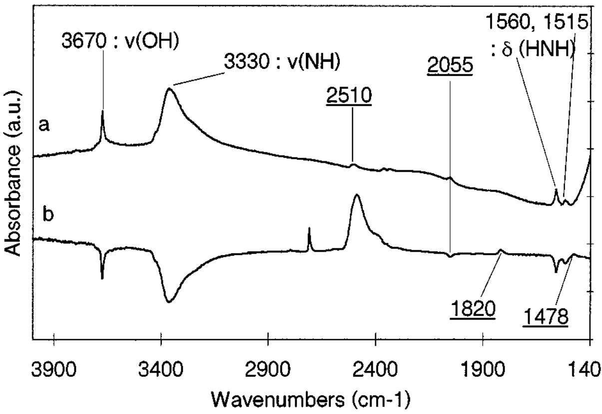

FIG. 2. (a) FTIR spectrum of the AlGaPON1 oxynitride after heating under hydrogen at 500°C. (b) Difference spectrum obtained after replacing hydrogen by deuterium at 500°C: spectrum recorded after deuterium adsorption—spectrum recorded after hydrogen adsorption.

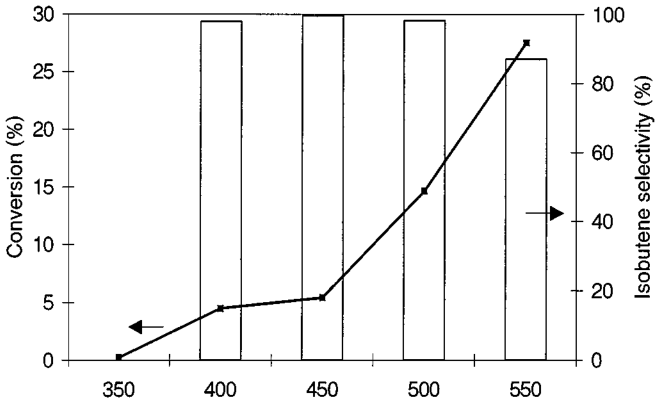

FIG. 3. Evolution of the isobutane conversion and isobutene selectivity as a function of temperature over the nonimpregnated AlGaPO sample (WHSV = 0.03 h^{-1} and $isoC_4/H_2 = 1/6$).

After dissolution—and possibly reaction—of the deposit with acetone, heavy molecular weight amide molecules were detected by mass spectrometry. The nature and formation mechanism of those nitrogen containing molecules need to be further investigated but their appearance suggests the possibility of using nitrided phosphates to catalyze reactions necessitating the incorporation of nitrogen atoms in a hydrocarbon skeleton.

TABLE 3

Influence of the Cationic Substitution of Aluminum by Gallium on the Catalytic Activity of Platinum-Impregnated Al(Ga)PO Phosphates (WHSV = 0.55 h^{-1}, $T = 500°C$, and $isoC_4/H_2 = 1/6$)

	Pt/AlPO	Pt/AlGaPO
Conversion (%)	58.9	49.7
Isobutene yield (%)	40.9	48.5
Selectivities (%)		
isobutene	69.4	97.5
methane	1.5	0.2
ethane	3.2	0.1
propane	2.0	0.1
ethylene	0.6	0[a]
propylene	2.0	0.2
n-butane	5.6	0.4
1-butene	4.2	0.4
trans-2-butene	5.9	0.6
cis-2-butene	4.3	0.4
1,3-butadiene	1.4	0[a]

[a] Traces.

Influence of the cationic substitution of aluminum by gallium. Comparison of the catalytic activities of Pt/AlPO and Pt/AlGaPO samples (Fig. 4) clearly demonstrates that the substitution of a fraction of the aluminum atoms by gallium modifies the catalytic properties of the platinum-impregnated phosphates. Two effects must be taken into account when comparing the results obtained at 500°C on the Pt/AlPO and Pt/AlGaPO samples after a progressive temperature rise, namely the role of gallium on the activity and stability of the catalysts. To distinguish these two effects, the initial activities of the two samples were measured directly at 500°C, then their stability was evaluated for 19 h on stream. The tests were conducted at a WHSV of 0.55 h^{-1}. A this higher WHSV, errors on the mass balance did not exceed 3.5%.

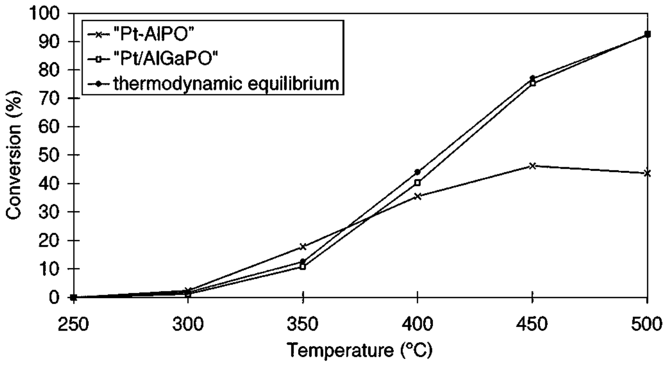

FIG. 4. Evolution of the isobutane conversion as a function of temperature over platinum-impregnated AlPO and AlGaPO samples (WHSV = 0.03 h^{-1} and $isoC_4/H_2 = 1/6$); calculated thermodynamic values are also shown.

Under the new operating conditions, the calculated thermodynamic equilibrium was 72%.

Table 3 presents the conversions obtained on the Pt/AlPO and Pt/AlGaPO samples after 2 min. on stream at 500°C, as well as the selectivities for the various reaction products. On the Pt/AlPO, selectivity for isobutene is 69%, but the analysis of all the reaction products indicates that other catalytic functions are also present. Next to isobutene, one finds hydrogenolysis, cracking, and isobutene isomerization products. The existence of cracking and secondary isomerization products could be attributed to the existence of some relatively strong acid sites on the support, which have been evidenced by ammonia chemisorption experiments (22). Observation of the reaction products on the Pt/AlGaPO is evidence that the substitution of aluminum by gallium markedly increases the selectivity of the transformation to isobutene, which reaches 98%. Correlatively, selectivities to lighter C_1–C_3 and isomerization products are very low for the gallium-containing sample.

The evolution of the conversions with time on stream is presented in Fig. 5 for the two tested catalysts. For both samples, the conversion progressively decreases with time on stream and does not seem to reach a stationary state, even after 19 h.

This activity decrease cannot be attributed to a surface area decrease during the reaction, since it is relatively stable at 500°C (relative surface area decrease <5% after 19 h of test), but it could be attributed to the formation of carbonaceous deposits on the surface. Indeed, chemical analyses

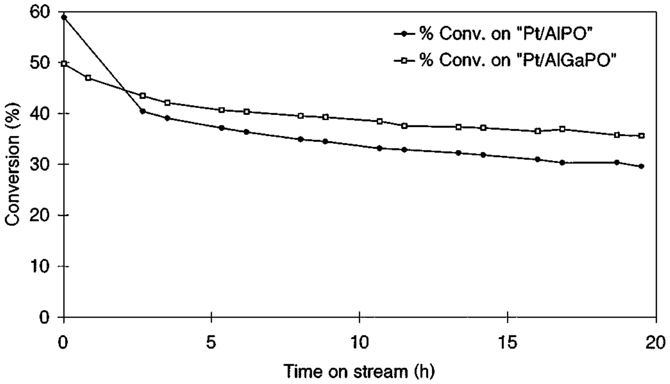

FIG. 5. Evolution of the conversion with time on stream for the Pt/AlPO and Pt/AlGaPO samples (WHSV = 0.55 h^{-1}, $T = 500°C$ and iso$C_4/H_2 = 1/6$).

performed before and after the test indicate a deposition of carbon on the surface during time on stream (23).

However, gallium also reduces the catalyst deactivation rate; the absolute conversion decrease after 19 h is much higher for the Pt/AlPO sample (28%) than for the Pt/AlGaPO sample (14%).

Influence of the anionic substitution of oxygen by nitrogen. The conversions and isobutene yields obtained after 2 min on stream on the Pt/AlGaPO, Pt/AlGaPON1, and Pt/AlGaPON2 samples are presented in Table 4. Conversions normalized to identical specific surface areas are also shown. We think indeed that the specific surface area of the support is of importance when comparing series of samples with increasing nitrogen contents. As will be detailed in the Discussion, we propose that some active sites are localized on the support.

Comparison of the results indicates that although substitution of nitrogen in the phosphate network considerably reduces the catalyst specific surface areas (Tables 1 and 2), it has a positive effect on the conversion. This conversion increase is accompanied by a small decrease of the isobutene selectivity but, as can be seen in Table 4, nitridation has a global positive effect on the isobutene yield.

The role of nitridation on the conversion and yield is more pronounced for the most nitrided sample Pt/AlGaPON2. It should not be attributed to a modification of the impregnation process induced by nitrogen as dispersions on both Pt/AlGaPO and Pt/AlGaPON2 are very low (<2%).

The values of the absolute conversion decrease after 19 h on stream are also shown. Although conversions increase when oxygen is substituted by nitrogen, the conversion loss diminishes with the nitrogen enrichment. This suggests that nitridation of the support leads to a decrease of the catalyst deactivation rates.

Since it is known that AlGaPON oxynitrides lose nitrogen as gaseous ammonia at high temperature (24), the relative nitrogen loss after 19 h on stream at 500°C was evaluated for the Pt/AlGaPON2 sample. Elemental nitrogen analyses carried out prior to and after the test indicate a relative nitrogen loss of 7% during the course of the reaction. Hence, regenerative treatments of the impregnated nitrided samples would probably necessitate a renitridation of the catalysts, as well as the removal of the carbonaceous species deposited on the surface.

Influence of the hydrogen partial pressure on the catalytic activity and stability. In all the catalytic tests presented up to now, hydrogen was added to the reaction mix—the isobutane/hydrogen ratio being 1/6—in order to avoid coke formation and catalyst deactivation. This effect of the hydrogen partial pressure in the feed on the catalysts is illustrated in this last section. Four sets of reactions, presented in Table 5, were used on the Pt/AlGaPON2 catalyst. The isoC_4/H_2 molar ratios were changed from 1/40 to 1/0.4, while maintaining a constant total flow rate of 0.54 ml/mg.min (WHSV = 0.55 h^{-1}).

Table 6 presents the conversions and product distributions measured at 500°C after 2 min on stream for the four sets of reactions. To facilitate the subsequent discussion, we simplified the presentation of the results by combining methane, ethane, propane, ethylene, and propylene in the "C_1–C_3" selectivity term, and (un)saturated isomers in the "isomerization" selectivity term. Comparison of the initial

TABLE 4

Influence of the Anionic Substitution of Oxygen by Nitrogen on the Catalytic Activity of Platinum-Impregnated AlGaPO(N) Catalysts (WHSV = 0.55 h^{-1}, $T = 500°C$, and iso$C_4/H_2 = 1/6$)

	Pt/AlGaPO	Pt/AlGaPON1	Pt/AlGaPON2
Nitrogen content (wt%) after impregnation	0	5.6	11.8
Initial conversion (%)	49.7	54.4	68.4
Conversion after 19 h on stream	35.9	43.3	58.1
Absolute conversion decrease (%)	13.8	11.1	10.3
Initial conversion/S_{BET} (%/m^2)	0.22	0.35	0.53
Isobutene selectivity (%)	97.5	96.9	90.1
Isobutene yield (%)	48.5	52.7	61.6

TABLE 5

Effect of the Hydrogen Partial Pressure on the Catalytic Activity

Partial pressure	(total pressure = 1 atm)		$\approx$isoC$_4$/H$_2$	Total flow rate
(atm) Isobutane	Hydrogen	Helium	Molar ratios	(ml/min · mg)
0.7×10^{-2}	28.7×10^{-2}	0.706	1/40	0.54
0.7×10^{-2}	4.3×10^{-2}	0.950	1/6	0.54
0.7×10^{-2}	1.4×10^{-2}	0.979	1/2	0.54
0.7×10^{-2}	0.3×10^{-2}	0.990	1/0.4	0.54

activities measured for the four sets of reactions shows that the decrease of the hydrogen partial pressures is accompanied by an increase in the initial conversion, as well as an increased isobutene selectivity. However, when the hydrogen partial pressure is low, the rate of deactivation increases markedly (Fig. 6), which suggests that finding an optimal isobutane/H$_2$ molar ratio requires taking into account both the initial dehydrogenation and the deactivation rates.

Figure 7 shows that the evolution of the deactivation rate (Conv.$_{t=2\text{min}}$ (%) − Conv.$_{t=19\text{h}}$ (%)/19 (h)) as a function of the hydrogen partial pressure can be correlated to the amount of carbon deposited on the surface at the end of the reaction.

4. DISCUSSION

The mixed nitrided galloaluminophosphates AlGaPON constitute a nonconventional family of catalysts, with tuneable acid–base properties. They are obtained by ammonolysis of an amorphous mixed Al$_{0.5}$Ga$_{0.5}$PO$_4$ phosphate (19). This phosphate presents a marked acid character, due to the presence of surface Brønsted and Lewis acid sites. Pyridine adsorption experiments carried out on the precursor indicated that the presence of Brønsted acid sites was mainly due to the existence of surface P–OH species, while the presence of Lewis acid sites was attributed to coordinatively unsaturated Al^{3+} and Ga^{3+} ions (25, 26). Incorporation of nitrogen in the phosphate network leads to a decrease of the number of acid sites, and to the appearance of weak surface basic sites. Several publications were devoted to the identification of the basic sites on AlGaPON (27–29). It appears that the hydrogenated NH$_x$ species appearing upon nitridation are responsible for the basic properties of the nitrided samples, especially the −NH$_2$ species appearing by amination of the acidic P–OH groups.

TABLE 6

Conversions, Isobutene Yields, and Product Distributions Obtained on the Pt/AlGaPON2 Sample at 500°C as a Function of the isoC$_4$/H$_2$ Molar Ratio

$\approx$isoC$_4$/H$_2$ molar ratios	1/40	1/6	1/2	1/0.4
Conversion (%)	31.0	68.4	67.8	72.5
Isobutene yield (%)	28.0	61.6	63.5	69.0
Isobutene selectivity (%)	90.3	90.1	93.7	95.1
C$_1$–C$_3$ selectivity (%)	3.2	2.9	1.1	1.0
Isomerisation selectivity (%)	6.4	7.0	5.2	3.9

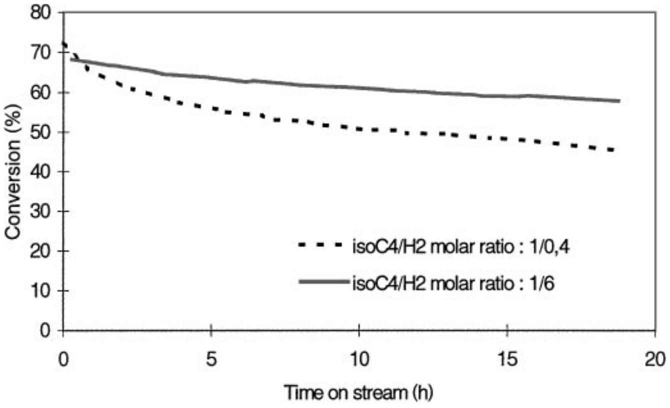

FIG. 6. Evolution of the conversion with time on stream for the Pt/AlGaPON2 tested for isobutane/H$_2$ ratios of 1/6 and 1/0.4 (T = 500°C, WHSV : 0.55 h^{-1}).

The ammonia temperature programmed desorptions carried out on the three AlGaPO, AlGaPON1, and AlGaPON2 samples prior to platinum impregnation illustrate the acidity decrease induced by nitridation (Table 1). The precursor adsorbs 7.7 μeq. NH$_3$/m^2, while the most nitrided sample only adsorbs 2.3 μeq. NH$_3$/m^2.

The best isobutene yields obtained in this work are those observed for the nitrided Pt/AlGaPON2 sample (62% at 500°C, see Table 4), which suggests that both gallium and nitrogen influence the catalytic properties of Pt/AlGaPON for the dehydrgenation of isobutane to isobutene.

We intend to propose some hypotheses relative to their role on the performances of the catalysts.

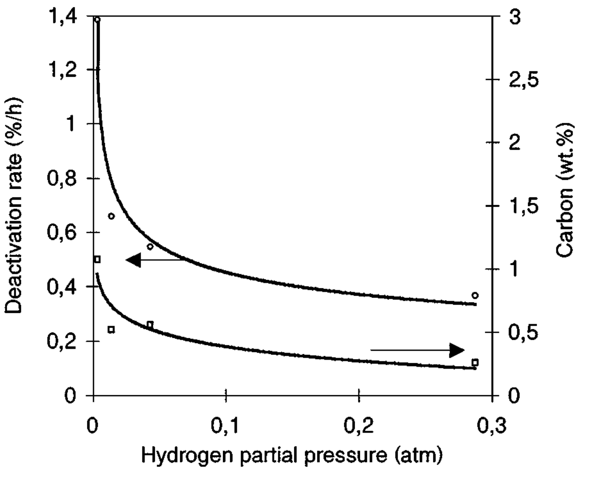

FIG. 7. Deactivation rate (○) and carbon deposition (□) as a function of the hydrogen partial pressure on the Pt/AlGaPON2 catalyst (WHSV = 0.55 h^{-1}, T = 500°C).

4.1. Catalytic Properties of Nonimpregnated AlPO and AlGaPO Samples

Under our operating conditions, the AlPO phosphate does not catalyze the dehydrogenation of isobutane to isobutene. However, substitution of half of the aluminium atoms by gallium allows the conversion of isobutane to isobutene, isobutene being detected when the temperature reaches 400°C (Fig. 3). This indicates that both C–H bond activation and release of H-atoms are possible on the AlGaPO phosphate.

This observation is consistent with the assumption of Meriaudeau et Naccache (30) that gallium is able to activate hydrocarbons as well as molecular hydrogen. They founded those assumptions (i) on the fact that gallium oxide Ga_2O_3 can selectively dehydrogenate short alkanes into the corresponding olefins, (ii) on the observation that reduced Ga_2O_3 is able to dissociate H_2 into H^+ and H^-; these two entities being observed by IR spectroscopy (31).

To determine whether Ga species in AlGaPON were similarly able to activate hydrogen, we studied the interactions of hydrogen with the surface by FTIR spectroscopy (Fig. 1). When the AlGaPON1 sample is evacuated at 500°C and then reduced at 500°C in hydrogen, two bands appear at 2055 and 2510 cm^{-1}.

The appearance of these bands can undoubtedly be attributed to the interaction of gallium atoms with molecular hydrogen.

The arguments are the following:

1. The bands are not visible on the AlGaPON1 sample evacuated at 500°C (except perhaps for a small shoulder around 2500 cm^{-1} (Fig. 1B)), but they appear when the sample is put in equilibrium with 0.16 atm of hydrogen.
2. The bands do not appear on a platinum-impregnated AlPON (3.8 wt% N after impregnation), which does not contain gallium, when it is reduced *in situ* at 500°C.
3. When, after reduction, the hydrogen is evacuated and replaced at 500°C by deuterium, the band at 2055 cm^{-1} is shifted at 1478 cm^{-1}, and the band at 2510 cm^{-1} is shifted at 1820 cm^{-1} (Fig. 2); the initial spectrum is restored after the evacuation of deuterium and its replacement by hydrogen. From this last result, it is obvious that the species giving rise to the two investigated IR bands contain hydrogen.

Bands at 2055 and 2510 cm^{-1} grow in parallel indicating that they correspond to species created simultaneously.

The band at 2055 cm^{-1} is likely due to the formation of Ga–H species (ν(Ga–H)), by analogy with the proposition of Meriaudeau *et al.* (31) that, on reduced gallium oxide, Ga^{x+}–H^- species give rise to an IR band around 2020 cm^{-1}.

The assignment of the second IR band at 2510 cm^{-1} is less clear; it has never been observed on AlGaPON samples. On phosphorus containing samples, a band in the 2800–2400 cm^{-1} region has already been reported. On P_2O_5 supported on silica, Low and Ramamurthy (32) detected a broad band at ∼2800 cm^{-1} and attributed it to hydroxyl groups associated to terminal P=O groups, in interaction with neighboring P=O groups, while the free ν(PO–H) vibration is observed at 3666 cm^{-1}. Stretching OH bands at such low frequencies would indicate a very strong hydrogen-bonding interaction. Bands in this low wavenumber zone were also observed on BPO_4 (at 2800–2760 cm^{-1}) (33) and on AlPON (34) (at 2500 cm^{-1}) and were ascribed to the same species. In our study, in contrast to what was observed on P_2O_5/SiO_2, the width of the band at 2510 cm^{-1} is not very large (∼25 cm^{-1}) and is similar to that of the band at 2055 cm^{-1}. This seems surprising for a band characteristic of perturbed OH groups. In our opinion, the attribution of the 2510 cm^{-1} band to a PH stretching vibration could also be considered since organophosphorus compounds give rise to a ν(P−H) band at 2450–2400 cm^{-1} (35).

Hence, even, if the attribution of the 2510 cm^{-1} band is not completely elucidated, we conclude that the Ga species present in the AlGaPON samples reduced at 500°C are able to dissociate H_2 into two entities visible at 2510 cm^{-1} (HO–P=O or H–P=O) and at 2055 cm^{-1} (Ga–H) on the IR spectra.

4.2. Catalytic Properties of Impregnated Samples

4.2.1. *Effects of the Substitution of Aluminum by Gallium*

The impregnation of both AlPO and AlGaPO samples with platinum results in a significant increase of their activity, indicating the fundamental role of platinum in the reaction, even if the dispersion of the metal on the surface is very low (Table 2). Platinum is known indeed to be a strong dehydrogenation agent.

However, the catalytic behavior of Pt/AlPO and Pt/AlGaPO is quite different (Table 3). The Pt/AlGaPO sample gives a much higher isobutene selectivity at 500°C, although conversions measured on both samples are quite similar. In addition, the deactivation rate of the Pt/AlGaPO is lower than that of the Pt/AlPO (Fig. 4).

Similar results in terms of isobutene selectivity and catalyst stability were obtained when comparing the catalytic properties of platinum-impregnated AlPON (13.6 wt%N after impregnation) and AlGaPON (5.6 wt%N after impregnation) samples at isoconversion (56 and 54% conversion, respectively). Tested at 500°C, at a WHSV of 0.55 h^{-1}, the Pt/AlPON converted isobutane to isobutene with a selectivity of 74%, the isobutene selectivity measured with the Pt/AlGaPON sample being of 97%. After 19 h on stream, the activity of the Pt/AlPON had decreased by 20%, the activity of the Pt/AlGaPON had decreased by only 11%.

At 500°C, the gallium contribution to isobutane dehydrogenation is poor and, in our opinion, the good selectivity of the Pt/AlGaPO sample suggests a synergy between platinum and gallium atoms rather than an additive action of platinum and gallium sites.

A synergy effect between platinum and gallium atoms was already proposed by Shpiro *et al.* (36) studying the *n*-butane aromatization on zeolites doubly promoted by gallium and platinum. They compared the catalytic properties of H-ZSM-5, Ga/H-ZSM-5, Pt/H-ZSM-5, and Pt-Ga/H-ZSM-5. They observed that the joint platinum and gallium introduction into H-ZSM-5 allowed one to increase the aromatization selectivity and the stability of the catalysts. They attributed the increase of the aromatization selectivity to the suppression of the hydrgogenolysis activity of platinum by gallium, platinum accelerating *n*-butane dehydrogenation, thereby decreasing the contribution of competitive cracking and isomerization reactions.

In their opinion, the suppression of the hydrogenolysis activity of platinum could be explained by both intimate interactions and long distance effect:

—Platinum and gallium can contact directly in mixed Pt–Ga particles, hence moderation of the platinum hydrogenolysis activity could be caused either by alloying of platinum and gallium, or by platinum decoration by gallium;

—Concerning the long distance effect, the authors invoke the ability of gallium species to perform back hydrogen spillover, which reduces the hydrogenolysis on platinum (as well as reducing hydrogenation).

The ability of gallium species to recombine hydrogen atoms to give H_2 is often invoked to explain the promoting effect of gallium on the aromatization properties of modified H-ZSM5 zeolites. This hypothesis is supported by the observation that the fraction of the hydrogen removed as H_2 during conversion of alkanes is much higher on samples containing gallium than on unpromoted H-ZSM5 (14).

Direct extrapolation of the findings by Shpiro *et al.* for the aromatization on Pt–Ga/H-ZSM-5 to dehydrogenation on Pt/AlGaPO would be hazardous, but their hypotheses are worth considering in our case. In particular, as our FTIR study of the interactions of H_2 with the surface suggests that Ga species facilitate H_2 dissociation, we can speculate—on the basis of the microscopic reversibility principle—that Ga species in Pt/AlGaPON also facilitate the recombination of dissociated hydrogen species.

4.2.2. Effects of the Substitution of Oxygen by Nitrogen

The isobutane conversion increases when replacing oxygen by nitrogen in the phosphate network of the support in parallel with the isobutene yield (Table 4). This increase can be linked to the changes induced by the nitridation treatment on the support acid–base properties (see Table 1 and Refs. (25–29)). It is known that the catalytic properties of metal-supported catalysts are strongly influenced by this parameter. In the *n*-heptane conversion over supported platinum acid–base ZrPON catalysts, for instance, the catalytic activity and aromatization selectivity increases when the nitrogen content of the support increases, in parallel with the number of basic sites (37). It has been shown that the hydrogenation–dehydrogenation activity of platinum supported on zeolites strongly depends on their acido-basicity, the dehydrogenation being favored on basic supports, with the hydrogenation activity varying in the opposite direction (38).

The increased dehydrogenation activity of platinum clusters supported on basic zeolites is often attributed to metal–support interactions resulting from an electron transfer from highly negatively charged framework oxygen to the metal particles.

The adsorption coefficient of the unsaturated hydrocarbons being smaller on electron-rich particles, those electron transfers could favor the fast desorption of the products and hence higher turnovers (38).

Metal–support interactions can be demonstrated by the characterisation of the $\nu(CO)$ stretching frequency of adsorbed carbon monoxide (39–42). An electron excess of the metal results in a shift of the $\nu(CO)$ infrared band of linearly adsorbed CO to lower wavenumbers.

A priori metal–support interactions could also be invoked to explain the changes induced by nitridation on the dehydrogenation properties of Pt/AlGaPON. However, we tend to discard this hypothesis:

(i) Electronic interactions between platinum and basic sites on zeolites are described for very small platinum particles (i.e., for high platinum dispersions), and the same applies for the interactions between platinum and aluminum-stabilized magnesium oxide Mg(Al)O, a nonmicroporous basic support. This was demonstrated by Kazansky *et al.* (40, 41) who synthesized a Pt/Mg(Al)O catalyst for the selective aromatization of *n*-alkanes, with a platinum dispersion of 62%. Using diffuse reflectance IR spectroscopy of CO adsorption, Kazansky *et al* . showed that two different kinds of platinum particles—small and large clusters—existed on the surface of the catalysts. The small platinum clusters have unusual properties, like those found for Pt- loaded alkaline and alkaline-earth forms of zeolites, while larger clusters behave in a normal way toward the adsorption of CO (40).

In view of the low dispersions of platinum on AlGaPON, we expect the presence of large platinum agglomerates on the surface, rather than small platinum clusters. In that sense, we can refer to scanning electron microscopy (SEM) analysis performed by Centeno *et al.* (43) on a series of Pt/AlPO(N) samples, with platinum dispersions varying from 1.5 to 29.2%. The SEM micrographs revealed a regular distribution of platinum particles with an average size of 20 nm, with some agglomerates of about 1 μm on the best dispersed catalyst (29.2%). When the dispersion decreased, the amount of those large agglomerates increased.

(ii) A preliminary IR study of adsorbed CO on various Pt/AlPON and Pt/AlGaPON samples (complicated by the very low platinum dispersions) did not reveal changes in the ν(CO) stretching frequency with the nitrogen enrichment.

We thus propose a second hypothesis for the role of nitridation on the catalytic properties of Pt/AlGaPON. We suggest that nitridation induces the appearance of juxtaposed weakly acid and basic sites able to activate the isobutane molecule, a proton being abstracted on a basic site and the anionic product of this C–H bond activation being stabilized by the adjacent acid site. Examples of acid–base bifunctional effects have been discussed in a review by Iglesia *et al.* (8) presenting the unusual catalytic properties of amphoteric oxides for hydrogenation, dehydrogenation, and dehydration reactions.

In the case of Pt/AlGaPON, platinum (and possibly gallium) would increase the rate of this acid–base catalysis by providing a “porthole” for hydrogen desorption.

At this stage, the proposed reaction mechanism is still hypothetical, but in order to clarify our proposition, it is presented in Fig. 8.

We propose that isobutane can be dehydrogenated to isobutene either on the platinum particles or on the support or on juxtaposed acid–base sites; this second assumption explains the activity increase observed when more basic sites are created on the surface. In a final step, the surface of the catalyst would be regenerated by formation of gazeous hydrogen. The recombination of the H^+ and H^- species formed on the support occurs most probably on the platinum sites, but also possibly (see section 4.2.1.) on gallium sites. The nature and location of the gallium and platinum sites still needs to be determined.

The greater activities and stabilities of the gallium-containing samples compared to Pt/AlPO(N) suggest synergies between platinum and gallium that do not appear in this scheme but which have been discussed in Section 2.1.

Although the positive role of nitrogen on the isobutene yields is indisputable when platinum impregnated samples are used, we failed to demonstrate it on nonimpregnated samples. Conversions obtained on the nonimpregnated AlGaPON1 sample were significantly smaller than on the nonimpregnated AlGaPO (8% conversion at 550°C for a WHSV of 0.03 h^{-1}). Although we feel that this discrepancy could be caused by differences in the rate limiting step, we are not yet able to give a satisfactory explanation for the differences observed between impregnated and nonimpregnated samples.

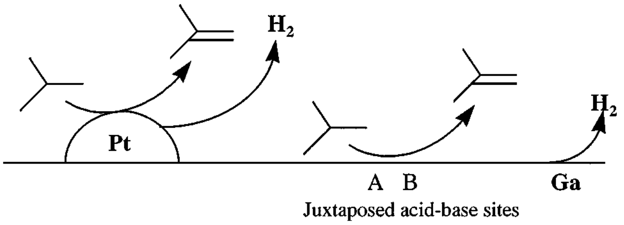

FIG. 8. Hypothetical representation of the isobutane dehydrogenation on the surface of Pt/AlGaPON.

TABLE 7

Carbon Deposition Analysis Performed on the Platinum-Impregnated Samples before and after the Test

	wt%C before test	wt%C after test	wt%C after— wt%C before test
Pt/AlGaPO	1.0	3.1	2.1
Pt/AlGaPON1	0.8	1.2	0.4
Pt/AlGaPON2	0.5	0.6	0.1

Note. T : 500°C, WHSV : 0.55 h^{-1}, test duration : 19 h.

Another role of nitrogen in Pt/AlGaPON is to reduce deactivation (Table 4), possibly because decreasing the acidity slows down the reactions leading to the formation of highly unsaturated molecules on the surface. In that sense, chemical analyses performed before and after the test indicate a greater deposition of carbon on the surface on the Pt/AlGAPO sample than on the Pt/AlGAPON samples (Table 7).

4.2.3. *Influence of the Hydrogen Partial Pressure*

As can be seen in Table 6, the hydrogen partial pressure in the feed strongly influences the Pt/AlGaPON activity and selectivity for the various reaction products. The activity increases when decreasing the hydrogen partial pressure, probably because it decreases the hydrogen surface coverage, shifting the equilibrium to the isobutene formation. At the same time, selectivities for lighter (C_1–C_3) products and isomers decrease. A similar effect is observed when the dehydrogenation of isobutane is carried out over Pt/Al_2O_3 or Cr_2O_3-Al_2O_3 catalysts in hydrogen-permeable membrane reactors. In those reactors, the removal of hydrogen suppresses undesirable side reactions, such as hydroisomerization and hydrogenolysis leading to high selectivity of isobutene. (44)

Deactivation rates, as well as the amount of carbon deposited on the surface at the end of the reaction, are also strongly dependent on the hydrogen partial pressure. Both decrease when increasing the hydrogen partial pressure (Fig. 7). This result was expected, since hydrogen has a negative effect on the conversion. But it is also in line with the behavior of a typical supported platinum catalyst, for which the deactivation rate is usually inversely proportional to the hydrogen concentration; the carbonaceous deposits on the surface are partially removed by reaction with hydrogen (6).

CONCLUSION

The dehydrogenation of isobutane to isobutene over various phosphates and nitrided phosphates impregnated or not with platinum has been studied. In a first step, it has been shown that isobutane is converted to isobutene on a mixed galloaluminophosphate AlGaPO, which reveals that both C–H bond activation and disposal of H atoms are possible on this type of gallium-containing solid. In a second step, this sample was used as a support for platinum and its activity was compared to that of a platinum-impregnated aluminophosphate. Higher isobutene yields were obtained on the gallium-containing catalyst, which also proved to be more stable with time.

One hypothesis ventured to explain the particular reactivity of the platinum impregnated AlGaPO was, by analogy with the results obtained by Shpiro *et al.* (36) on Pt/Ga zeolites, a synergetic effect between gallium and platinum atoms: the ability of gallium to recombine hydrogen in the molecular form during the reaction thereby decreasing the hydrogenolysis reactions over platinum aggregates. However, we could not provide a definitive experimental proof of the occurrence of this phenomenon on (Pt)AlGaPO(N).

Incorporating nitrogen in the phosphate network also contributes to improve the catalytic performances: it increases the isobutene yield and the catalyst stability.

The improved activity and stability of the Pt/AlGaPON samples, compared to the Pt/AlGaPO sample, is a good illustration that nitridation of amorphous phosphates is a way to enlarge the range of available heterogeneous catalysts worth investigating.

ACKNOWLEDGMENTS

The authors are grateful to the Fonds National de la Recherche Scientifique (FNRS) for the financial support and the fellowship awarded to Stéphanie Delsarte. They are also grateful to Jean Lamotte (Laboratoire de Catalyse et Spectrochimie, Caen, France) for the help provided in the recording and interpretation of the FTIR spectra of adsorbed hydrogen, deuterium, and carbon monoxide. They also thank F. Thyrion (Unité des procédés, Louvain-la-Neuve, Belgium) for the thermodynamic calculations performed in his laboratory.

REFERENCES

1. Morgan, M. L., *in* “Proceedings of the DGMK Conference, C_4 Chemistry—Manufacture and Use of C_4 Hydrocarbons” (W. Keim, B. Lücke, and J. Weitkamp, Eds.), Tagungsbericht 9705, p. 9. Germany, 1997.
2. Gullick, R. W., and Le Chevallier, M. W., *J. Am. Water Works Assoc.* **92**, 100 (2000).
3. Kogan, S., Herskowitz, M., Woerde H. M., and van den Oosterkamp, P. F., *in* “Proceedings of the DGMK Conference, C_4 Chemistry—Manufacture and Use of C_4 Hydrocarbons” (W. Keim, B. Lücke, and J. Weitkamp, Eds.), Tagungsbericht 9705, p. 117. Germany, 1997.
4. Cavani, F., Koutyrev, M., Trifiro, F., Bartolini, A., Ghisletti, D., Iezzi, R., Santuccini, A., and Del Piero, G., *J. Catal.* **158**, 236 (1996).
5. Lane, G. S., Modica, F. S., and Miller, J. T., *J. Catal.* **129**, 145 (1991).
6. Resasco, D. E., Marcus, B. K., Huang, C. S., and Durante, V. A., *J. Catal.* **146**, 40 (1994).
7. Imai, T., and Hung, C. W., U.S. Patent 4,430,517 (1983).
8. Iglesia, E., Barton, D. G., Biscardi, J. A., Gines, M. J. L., and Soled, S. L., *Catal. Today* **38**, 339 (1997).
9. Conanec, R., Marchand, R., and Laurent, Y., *High Temp. Chem. Processes* **1**, 157 (1992).
10. Grange, P., Bastians, P., Conanec, R., Marchand, R., and Laurent, Y., *Appl. Catal. A: Gen.* **114**, L191 (1994).
11. Grange, P., Bastians, P., Conanec, R., Marchand, R., Laurent, Y., Gandia, L., Montes, M., Fernandez, J., and Odriozola, J. A., *in* “Studies in Surface Science and Catalysis—91, Preparation of Catalysts VI” (G. Poncelet *et al.*, Eds.), p. 381. Elsevier, Amsterdam, 1995.
12. Guéguen, E., Kartheuser, B., Conanec, R., Marchand, R., Laurent, Y., and Grange, P., *in* “Proceedings of the DGMK Conference, Catalysis on Solid Acids and Bases” (J. Weitkamp and B. Lücke, Eds.), Tagungsbericht 9601, p. 235. Germany, 1996.
13. Kartheuser, B., Guéguen, E., Massinon, A., and Grange, P., *in* “Proceedings of the DGMK Conference, Catalysis on Solid Acids and Bases” (J. Weitkamp and B. Lücke, Eds.), Tagungsbericht 9601, p. 269. Germany, 1996.
14. Meitzner, G. D., Iglesia, E., Baumgartner, J. E., and Huang, E. S., *J. Catal.* **140**, 209 (1993).
15. Nakamura, I., and Fujimoto, K., *Catal. Today* **31**, 335 (1996).
16. Mowry, J. R., Anderson, R. F., and Johnson, J. A., *Oil Gas J.* **83**, 1288 (1985).
17. Courty, Ph., Ajot, H., Marcilly, Ch., and Delmon B., *Powder Technol.* **7**, 21 (1973).
18. Kearby, K., *in* “Proceedings of the 2nd International Congress on Catalysis,” p. 2567. Technip, Paris, 1961.
19. Peltier, V., Conanec, R., Marchand, R., Laurent, Y., Delsarte, S., Guéguen, E., and Grange, P., *Mater. Sci. Eng. B.* **47**, 177 (1997).
20. Massinon, A., Odriozola, J. A., Bastians, Ph., Conanec, R., Marchand, R., Laurent, Y., and Grange, P., *Appl. Catal. A: Gen.* **137**, 9 (1996).
21. Centeno, M. A., and Grange, P., *J. Phys. Chem. B.* **103**(13), 2431 (1999).
22. Massinon, A., Conanec, R., Marchand, R., Laurent, Y., and Grange, P., *in* “Proceedings of the DGMK—Tagungsbericht 9601, Conference on Catalysis on Solid Acids and Bases” (J. Weitkamp and B. Lücke, Eds.), p. 211. Graphische Betriebe Petra Lange, Hamburg, 1996.
23. Delsarte, S., Laurent, Y., and Grange, P., *in* “Nitrides and Oxynitrides” (S. Hamphire and M. J. Pomeroy, Eds.), Vols. 325–326, p. 51. Trans Tech, Switzerland, 2000.
24. Centeno, M. A., Delsarte, S., and Grange, P., *J. Phys. Chem. B*, **103**(34), 7214 (1999).
25. Delsarte, S., Peltier, V., Laurent, Y., and Grange, P., *in* “Studies in Surface Science and Catalysis—118, Preparation of Catalysts VII” (B. Delmon *et al.*, Eds), p. 869. Elsevier, Amsterdam, 1998.
26. Delsarte, S., Ph.D. thesis, Université Catholique de Louvain, 2000.
27. Delsarte, S., and Grange, P., *in* “Studies in Surface Science and Catalysis—130, Proceedings of the 12th International Congress on Catalysis” (A. Corma *et al.*, Eds), p. 3237. Elsevier, Amsterdam, 2000.
28. Delsarte, S., Auroux, A., and Grange, P., *Phys. Chem. Chem. Phys.* **2**, 2821 (2000).
29. Delsarte, S., Maugé, F., Lavalley, J.-C., and Grange, P., *Catal. Lett.* **68**, 79 (2000).
30. Mériaudeau, P., and Naccache, C., *Catal. Today* **31**, 265 (1996).
31. Mériaudeau, P., and Primet, M., *J. Mol. Catal.* **61**, 227 (1990).
32. Low, M. J. D., and Ramamurthy P., *J Phys. Chem.* **72**, 3161 (1968).
33. Moffat, J. B., and Neeleman, J. F., *J. Catal.* **34**, 376 (1974) .
34. Benitez, J. J., Diaz, A., Laurent, Y., and Odriozola, J. A., *J. Mater. Chem.* **8**(3), 687 (1998).
35. Ferraro, J. R., *in* “Progress in Infrared Spectroscopy” (H. A. Szymanski, Eds.), Vol. 2, p. 134. Plenum Press, New York, 1964.

36. Shpiro, E. S., Shevchenko, D. P., Dmitriev, R. V., Tkachenko, O. P., and Minachev, Kh. M., *Appl. Catal. A*, **107**, 165 (1994).
37. Fripiat, N., and Grange, P., *Catal. Lett.* **62**, 53 (1999).
38. Barthomeuf, D., *Catal. Rev.-Sci. Eng.* **38**(4), 521 (1996).
39. de Mallmann, A., and Barthomeuf, D., *J. Chim. Phys.* **87**, 535 (1990).
40. Kazansky, V. B., Borovkov, V. Yu., and Derouane, E. G., *Catal. Lett.* **19**, 327 (1993).
41. Kazansky, V. B., Borovkov, V. Yu., Sokolova, N., Jaeger, N. I., and Schulz-Ekloff, G., *Catal. Lett.* **23**, 263 (1994).
42. Badri, A., Binet, C., and Lavalley, J. C., *J. Chem. Soc. Faraday Trans.* **92**(9), 1603 (1996).
43. Centeno, M. A., Debois, M., and Grange, P., *J. Catal.* **192**, 296 (2000).
44. Matsuda, T., Koike, I., Kubo, N., and Kikuchi, E., *Appl. Catal. A: Gen.* **96**, 3 (1993).